

 Open access • Journal Article • DOI:10.1039/C0LC00090F

Design of a compact microfluidic device for controllable cell distribution

— [Source link](#) 

Jingliang Li, Daniel Day, Min Gu

Institutions: Swinburne University of Technology

Published on: 27 Oct 2010 - Lab on a Chip (The Royal Society of Chemistry)

Related papers:

- [Preparation method for microfluidic array controller](#)
- [Centrifugal force-based microfluidic device available for reliability verification, and analyzing method using the same](#)
- [Microchambers flow simulation for immunoassay-based biosensing applications](#)
- [Microfluidic device and method for operating thereof](#)
- [Microfluidic Separation System Based on Image](#)

Share this paper:    

View more about this paper here: <https://typeset.io/papers/design-of-a-compact-microfluidic-device-for-controllable-cell-4qsbdlfw0s>

Deakin Research Online

This is the published version:

Li, Jing-Liang, Day, Daniel and Gu, Min 2010, Design of a compact microfluidic device for controllable cell distribution, *Lab on a chip*, vol. 10, no. 22, pp. 3054-3057.

Available from Deakin Research Online:

<http://hdl.handle.net/10536/DRO/DU:30039304>

Reproduced with the kind permission of the copyright owner.

Copyright : 2010, The Royal Society of Chemistry

Design of a compact microfluidic device for controllable cell distribution

Jing-Liang Li,* Daniel Day and Min Gu*

Received 11th June 2010, Accepted 2nd September 2010

DOI: 10.1039/c0lc00090f

A compact microfluidic device with 96 microchambers allocated within four circular units was designed and examined for cell distribution. In each unit, cells were distributed to the surrounding chambers radially from the center. The circular arrangement of the chambers makes the design simple and compact. A controllable and quantitative cell distribution is achievable in this device. This design is significant to the microfluidic applications where controllable distribution of cells in multiple microchambers is demanded.

Microfluidic devices have shown important advancements in various aspects of biology from cell culturing to advanced applications such as digital polymerase chain reaction (PCR),^{1,2} nanoparticle synthesis,³ nanoparticle-cell interactions⁴ and protein crystallization.⁵ The advantages of microfluidic devices over the traditional devices include miniaturization which requires the use of solvent/drugs with volumes only from pico to micro liters,^{6,7} continuous perfusion to provide better control over the environment for cell growth,⁸ and convenience in integration with electronic control.¹

In general, a microfluidic device for cell culturing purpose or cell-based assay requires multiple microchambers in a single assembly for quantitative and statistic study. One big challenge for this type of device is to quantitatively control the distribution of cells in each chamber. Generally, the microchambers of such a microfluidic device are designed to locate along parallel channels (Fig. 1a) with the aim of achieving equal resistance in the channels, a prerequisite for even flow in each chamber.^{6,9} This normally requires repeated splitting of channels. The disadvantages of this design include (a) it needs a large space to accommodate the microstructures when the number of chambers required is large, and (b) it is a challenge to ensure the homogeneity of the dimensions of channels when they are getting longer with an increase in the number of chambers. In addition, it is difficult to ensure symmetry due to repeated splitting, a big cause of uneven flow in parallel channels, which is major factor influencing the flow and cell distribution into different chambers. In addition, due to the low density of cells, allocating cells into chambers in a quantitatively controllable manner remains a challenge. To address this problem, several methods have been applied, which include the incorporation of cell trapping structures such as pillars and sieves to help physically retain cells in the chambers.¹⁰ However, incorporation of fine structures in the design often adds challenges to the fabrication process. In addition, the presence of these structures leads to pressure buildup, which is not beneficial to cell function. Thus, it is important to design simple microfluidic devices with good flow distribution and allowing an undisturbed (natural) settlement of cells. To this end, considerations have to be taken into the design that can

reduce multiple splitting and channel length, as well as eliminate the use of trapping structures. Allocation of microchambers in a circular pattern (Fig. 1b), which offers perfect symmetry and reduced distribution length, can be a good solution. However, such a design has not been reported to the best knowledge of the authors.

In this work, a microfluidic device with 96 microchambers allocated to four circular units are designed, with each having 24 chambers (Fig. 1c). Cells delivered to the center of each unit were distributed radially into the surrounding chambers. The short radial distance to the chambers can minimize the adverse effects of the dimension difference between channels on flow splitting and cell distribution. The circular arrangement of the microchambers also leads to a compact design of microfluidic devices. In this device, flow

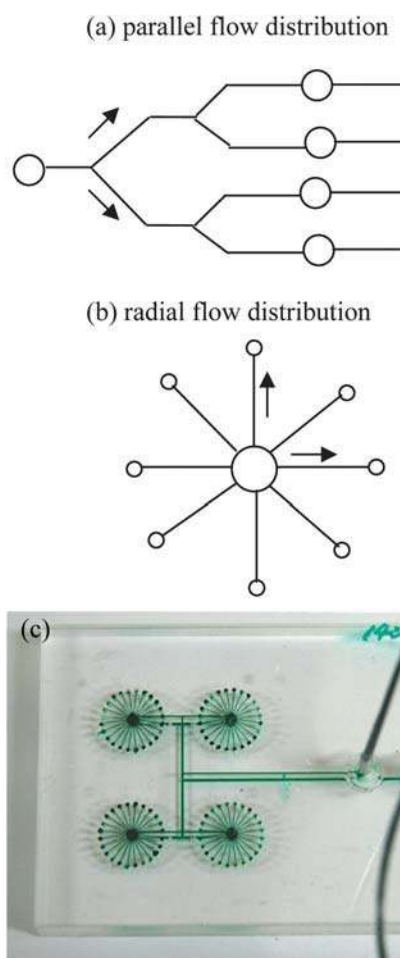


Fig. 1 Illustration of (a) parallel and (b) radial flow distribution and (c) a microfluidic device with radial flow distribution. The device is filled with a green food dye.

Centre for Micro-Photonics, Faculty of Engineering and Industrial Sciences, Swinburne University of Technology, Hawthorn, Victoria, 3122, Australia. E-mail: jili@swin.edu.au; mgu@swin.edu.au; Fax: +61 3 92145435; Tel: +61 3 92148776

in the microchambers is against the direction of gravitational force, which helps the settlement of cells. The large difference between the dimensions of the microchambers ($500\ \mu\text{m}$ diameter \times $2\ \text{mm}$ thickness) and channels ($70\ \mu\text{m}$ in diameter) also leads to the formation of “zero” flow areas, which is also conducive to the retaining of cells in the microchambers. These advantages ensures quantitative control over the number of cells in the microchambers.

The microstructures were fabricated in PMMA slides, which were then assembled by thermal bonding. PMMA slides ($76 \times 25 \times 2\ \text{mm}$) with a glass transition temperature around $90\ ^\circ\text{C}$ were obtained from Profile Plastics, Melbourne, Australia. A CO_2 laser (Versa Laser) with a work area up to $813 \times 475\ \text{mm}$ and a maximal power of 60 watts was used to fabricate the microstructures in PMMA slides. Compared with other techniques such as soft lithography, CO_2 laser micromachining provides a convenient way to fabricate microfluidic devices, since microstructures can be directly created on substrates.¹¹ Microstructures of the device were drawn using a Coreldraw software and then printed to the laser operating software. The slides were ultrasonically cleaned in isopropanol to remove the debris and then assembled by thermal bonding at $140\ ^\circ\text{C}$ for 7 min. A hotplate with temperature control was used for this purpose. The slides were pressurized with a self-made mechanical clamp. The pressure applied was controlled with a torque wrench. A torque of 4 Nm was applied, under which no channel blockage was observed after bonding. A schematic description of the microstructures fabricated on the slides and the flow directions are given in Fig. 2.

The capacity of the device to trap and distribute fluorescent polystyrene microbeads ($9.9\ \mu\text{m}$), which has a density similar to that of cells, was characterized. Fig. 3a and 3b show the transmission microscopic images of beads in two representative microchambers. By replacing the thick bottom PMMA layer of the device with a thin ($100\ \mu\text{m}$) PMMA slide/paper, the fluorescence of the beads can be imaged. Fig. 3(c) and (d) are the combined two-photon fluorescence and transmission images of beads trapped in two microchambers, which indicates that higher resolution fluorescence imaging can be achieved with the microfluidic device. This is important to advanced applications of the device such as for fluorescence-based cellular imaging. A quantitative distribution of beads in the microchambers was characterized using a diluted suspension of microbeads ($1.5 \times 10^5/\text{mL}$). The numbers of beads in the 24 chambers of a circular unit (A) are given in Fig. 3(e). The numbers of beads in the chambers are between 55 and 72, which is close to the homogeneous distribution. The calculated trapping efficiency is 92%. The numbers of beads in the other three units are 49–65 (B), 57–75 (C) and 53–76 (D). Although the radial distance to each chamber is short, slight heterogeneity in channel dimension can still cause difference in flow speed. This affects the number of beads deposited into each chambers. In addition, we noticed that it is difficult to make each microchamber the same size due to the fluctuation of laser intensity during the micromachining process. The distribution can be improved by optimizing the laser parameters to minimize the heterogeneity of the dimensions of channels and microchambers. It was observed a very small amount of beads (<5%) were retained in the channels, where the surface of channels is not smooth. This can also be further reduced by optimizing the laser parameters during the micromachining process. For cell culture, ways can be found to selectively modify the surface of the chambers for improved cell attachment, while leaving the channels untreated to prevent the sticking and proliferation of

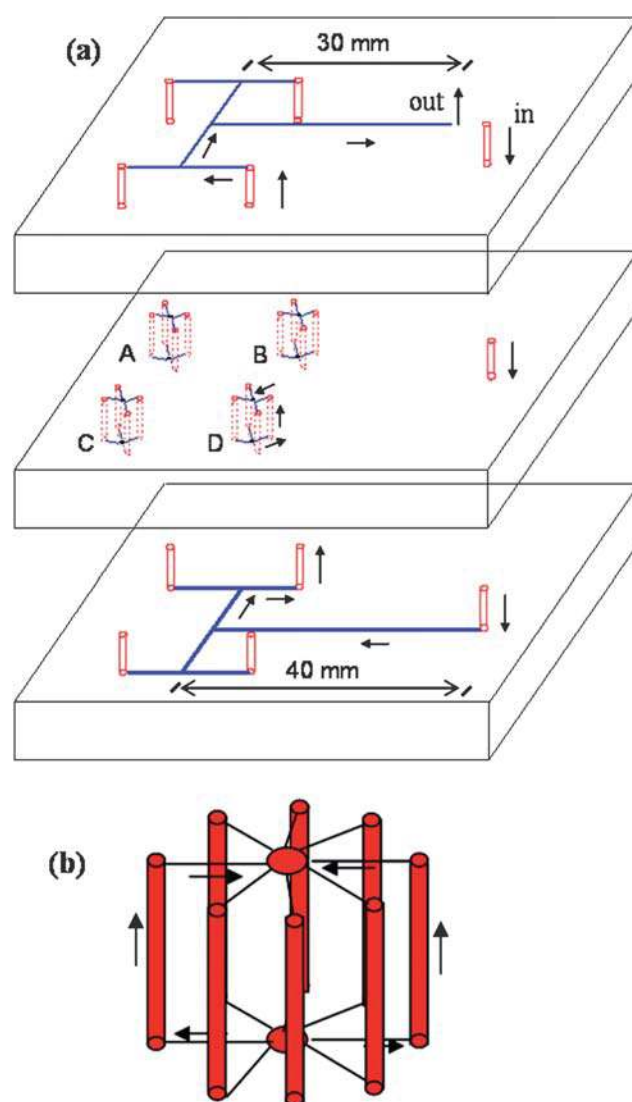


Fig. 2 (a) A schematic description of the design of the device. Line/curve in red means laser cutting through the slide, blue and black mean etching and raster on the surface, respectively, and (b) illustration of medium flow in one circular unit. On the bottom side, medium is distributed into microchambers from the center in the radial direction, which goes upwards and converges at the centre on the top side. The radial distance from the centre of a circular unit to the surrounding chambers is 5 mm; the distance between the centers of units A and B (C and D) are 15 mm, and that between A and C (B and D) is 30 mm.

cells in the channels. The smoothness can also be improved by using fabrication techniques such as electron beam lithography with a higher resolution other than CO_2 laser micromachining. While CO_2 laser micromachining is a simple method for the fabrication of microstructures, the resolution is not high. This low resolution makes CO_2 laser micromachining suitable to the fabrication of large structures only. By using other techniques that can provide higher resolution, not only the dimensions of channels and microchambers can be more homogeneous, but also the surface smoothness can be improved. This will improve the cell distribution and reduce retention in the channels.

A human cervical cancer cell line (HeLa) was used to test the capacity of this device for the quantitative cell distribution. HeLa cells

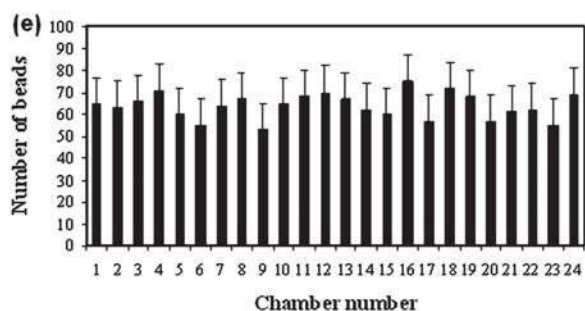
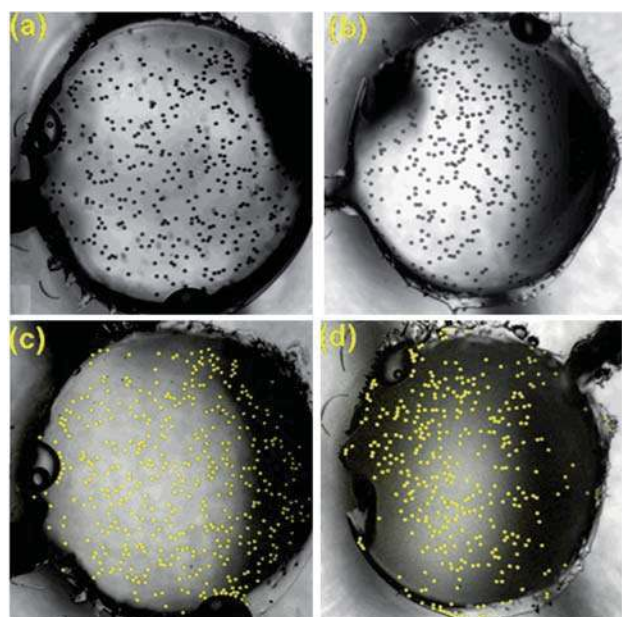


Fig. 3 Loading and imaging of microbeads in the microfluidic chambers. (a) and (b) are transmission images of microbeads, (c) and (d) are combined two-photon fluorescence and transmission images of microbeads when a 100 μm thick PMMA slide is used as the bottom layer of the device, (e) distribution of beads in the chambers of one circular unit of the microfluidic device.

were cultured in a RPMI medium supplied with fetal bovine (10%) serum at 37 $^{\circ}\text{C}$ under a 10% CO_2 atmosphere. Cells growing in a 25 cm^2 culture bottle were suspended with trypsin. Then the cell dispersion was centrifuged and the cells were redispersed in fresh medium. The chambers were filled with the cell suspension using a syringe slowly by hand with a flow rate at approximately 0.25 mL/min , which results in a flow rate of 2.6 $\mu\text{L}/\text{min}$ in each microchamber. The corresponding average cross sectional flow speed is 0.22 mm/s , which is about 2% of the speed in the distribution channels (the flow speed is reversely proportional to the cross section area). Since the injection takes only about 10 s, cell aggregation can be minimized, which ensures uniform cell concentration during cell loading. After the cells settled, the number of cells in each chamber was quantified. It was observed that most cells in the flow can stay in the microchambers due to the significantly reduced flow speed in the chambers. In addition, the flow in the anti-gravitational direction and the large depth of the chambers (2 mm) is also conducive to the settling of cells. The loading efficiency of cells in the chambers was characterized. When the concentration of cells in influent was 3.6×10^5 cells/mL, the

concentration in the effluent was found to be 3×10^4 , which means a high efficiency of over 90% for cell loading can be achieved. It is possible that the loading efficiency can be further improved by reducing the flow rate using a syringe pump. It is worth mentioning that the suitable flow rates depend on the dimension of the microchambers and channels. A too slow flow will increase the chance of cell sticking to the channels and sticking of cells to each other, lowering the loading efficiency and cell distribution quality. When the flow rate is too high, the pressure buildup may not be good to cells. In our work, a fast flow rate (hand injection) (> 0.5 mL/min) led to quick pressure buildup, which cause disconnection of inlet tubing. The high efficiency of cell loading means that we can control the number of cells in the chambers by simply varying the concentration of cells in the influent or by varying the volume of cell suspension at a fixed cell concentration. Fig. 4(a) and 4(b) displays the cells in a representative chambers at two different cell concentrations. The concentration of the cells in the influent in case of Fig. 4(b) (1×10^5 cells/mL) is ten times of that in Fig. 4(a) (1×10^4 cells/mL). The number of cells in Fig. 4(b) is 44, while that in Fig. 4(a) is 5. That is, the number of cells in Fig. 4(b) is about ten times of that in Fig. 4(a), which is corresponding to the ratio of the cell concentrations in the

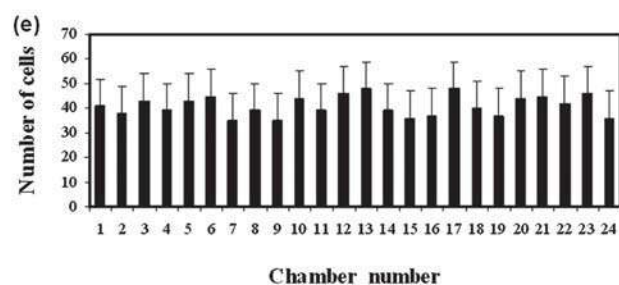
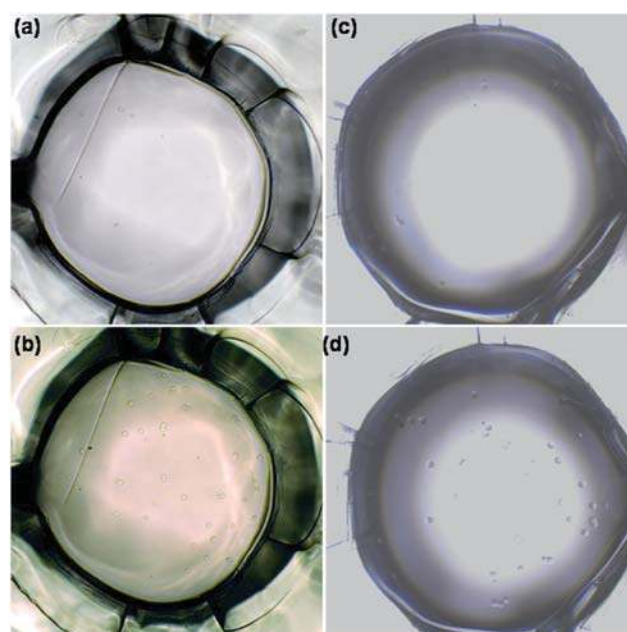


Fig. 4 Low density (a and c) and high density (b and d) cell trapping in two representative microchambers by controlling the concentration of cells in the influent, as well as distribution of cells in a representative circular unit for the high density cell loading (e).

loading solutions. Fig.4(c) and 4(d) are the corresponding pictures of cells in another microchambers at the low and high cell loading densities. A histogram of the cell distribution in the 24 chambers of a representative circular unit (A) under the high density cell loading is given in Fig. 4(e), with a range of 35–48 cells in the microchambers. The distribution of cells in the other three circular units is similar, which are 32–47 (B), 39–50 (C) and 40–54 (D).

In summary, a compact microfluidic device with circularly arranged microchambers was designed for radial distribution of microbeads and cells into each chamber. This pattern of microchamber arrangement can make the design more compact and reduce the resistance of channels, which is important when a large quantity of microchambers is needed in a single microfluidic device. A quantitative distribution of cells in the microchambers can be achieved in this device easily by controlling the concentration of cells in the flow. However, it is not recommended to use very high input cell concentration when the required number of cells in the microchamber is high. This will make the deposit of a monolayer of cells a challenge, because cells tend to stick quickly when their concentration is high. Since the trapping of cells is achieved by reduced flow and gravitational force in the microchambers, the number of cells can also be controlled by adjusting the volume of the input cell suspension while using a low or moderate cell concentration. The ideal range of cell concentration should be based on the dimension of the microchambers. In this work, a concentration not higher than 5×10^5 cells/mL is good to achieve well distributed cells in the microchambers.

The design of the radial flow distribution can be readily applied to materials other than the PMMA used in this work with suitable fabrication techniques. It is expected that long term cell culture can be achieved by suitable surface functionalization of the substrate. Consideration can also be given to the fabrication of such a device with gas permeable materials such as PDMS. The use of this type of material can eliminate the necessity of continuous perfusion of the system during cell culturing, making the application of this device more convenient. To this end, a combination of PMMA and PDMS can also be considered. In addition, while it is not possible to vary the flow into the microchambers of a circular unit, incorporating valves in the design will make it achievable to deliver species of different types and concentrations to different circular units (and the microchambers within), allowing for the culturing of cells under different chemical environments achievable with a single device.

Acknowledgements

The authors acknowledge the Cooperative Research Centre for Polymers (CRC-Polymer) of Australia for the financial support.

Notes and references

- 1 G. M. Whitesides, *Nature*, 2006, **442**, 368–373.
- 2 E. Leclerc, Y. Sakai and T. Fujii, *Biomed. Microdevices*, 2003, **5**, 109–114; E. A. Ottesen, J. W. Hong, S. R. Quake and J. R. Leadbetter, *Science*, 2006, **314**, 1464–1467.
- 3 K. S. Huang, T. H. Lai and Y. C. Lin, *Lab Chip*, 2006, **6**, 954–957; L. H. Hung, K. M. Choi, W. Y. Tseng, Y. C. Tan, K. J. Shea and A. P. Lee, *Lab Chip*, 2006, **6**, 174–178; R. Karnik, F. Gu, P. Basto, C. Cannizzaro, L. Dean, W. Kyei-Manu, R. Langer and O. C. Farokhzad, *Nano Lett.*, 2008, **8**, 2906–2912.
- 4 O. C. Farokhzad, A. Khademhosseini, S. Y. Yon, A. Hermann, J. J. Cheng, C. Chin, A. Kiselyuk, B. Tepy, G. Eng and R. Langer, *Anal. Chem.*, 2005, **77**, 5453–5459.
- 5 D. Mark, S. Haeberle, G. Roth, F. von Stetten and R. Zengerle, *Chem. Soc. Rev.*, 2010, **39**, 1153–1182; S. Marre and K. F. Jensen, *Chem. Soc. Rev.*, 2010, **39**, 1183–1202; D. Chatterjee, A. J. Ytterberg, S. U. Son, J. A. Loo and R. L. Garrell, *Anal. Chem.*, 2010, **82**, 2095–2101.
- 6 J. S. Marcus, W. F. Anderson and S. R. Quake, *Anal. Chem.*, 2006, **78**, 956–958.
- 7 P. J. Lee, P. J. Hung, V. M. Rao and L. P. Lee, *Biotechnol. Bioeng.*, 2006, **94**, 5–14; D. Huh, K. L. Mills, X. Y. Zhu, M. A. Burns, M. D. Thouless and S. Takayama, *Nat. Mater.*, 2007, **6**, 424–428; L. Li, W. B. Du and R. F. Ismagilov, *J. Am. Chem. Soc.*, 2010, **132**, 112–119.
- 8 P. J. Hung, P. J. Lee, P. Sabounchi, R. Lin and L. P. Lee, *Biotechnol. Bioeng.*, 2005, **89**, 1–8; E. W. K. Young and D. J. Beebe, *Chem. Soc. Rev.*, 2010, **39**, 1036–1048.
- 9 E. Figallo, C. Cannizzaro, S. Gerecht, J. A. Burdick, R. Langer, N. Elvassore and G. Vunjak-Novakovic, *Lab Chip*, 2007, **7**, 710–719; D. N. Adamson, D. Mustafi, J. X. J. Zhang, B. Zheng and R. F. Ismagilov, *Lab Chip*, 2006, **6**, 1178–1186; J. Wang, Z. Y. Chen, M. Mauk, K. S. Hong, M. Y. Li, S. Yang and H. H. Bau, *Biomed. Microdevices*, 2005, **7**, 313–322; D. B. Weibel and G. M. Whitesides, *Curr. Opin. Chem. Biol.*, 2006, **10**, 584–591.
- 10 Z. H. Wang, M. C. Kim, M. Marquez and T. Thorsen, *Lab Chip*, 2007, **7**, 740–745; H. H. Cui and K. M. Lim, *Langmuir*, 2009, **25**, 3336–3339; L. Zhu, X. L. Peh, H. M. Ji, C. Y. Teo, H. H. Feng and W. T. Liu, *Biomed. Microdevices*, 2007, **9**, 745–750; M. C. Kim, Z. H. Wang, R. H. W. Lam and T. Thorsen, *J. Appl. Phys.*, 2008, **103**, 044701.
- 11 H. Y. Tan, W. K. Loke, Y. T. Tan and N. T. Nguyen, *Lab Chip*, 2008, **8**, 885–891; S. C. Wang, C. Y. Lee and H. P. Chen, *J. Chromatogr., A*, 2006, **1111**, 252–257; M. H. Yen, J. Y. Cheng, C. W. Wei, Y. C. Chuang and T. H. Young, *J. Micromech. Microeng.*, 2006, **16**, 1143–1153.